Bulletin of JSME, Vol. 28, No. 239, May 1985

Paper No. 239—10

Study of a Piston Pump without Valves*

(2nd Report, Pumping Effect and Resonance in a Pipe-capacity-system with a T-junction)

By Shoji TAKAGI**, Keiju TAKAHASHI***

This paper is concerned with a piston pump without valves which consists of a piping system with a T-junction, two capacities connected with both ends of the main pipe, and a piston installed in the lateral pipe. Pumping effect is examined theoretically and experimentally. The study is confined to the case that the time average flow in the main pipe is zero. The effect of resonance phenomena on the pump characteristics was clarified. The effect of system parameters on the pump characteristics was also clarified. The analytical results obtained from a mathematical model proposed in this paper were found to be good agreement with the experimental data.

Key Words : Fluid Vibration, Unsteady Flow, Pump, Resonance, Bio-mechanics, T-junction

1. Introduction

Several papers were reported on piston pumps without valves which were related to the phenomena in blood circulation system[(1)~(5)]. In a previous paper[(6)], one of the authors discussed the mechanism of the pumping effect of a piston pump without valves which consists of rigid pipes with a T-junction, two tanks with a large cross sectional area installed at both ends of the main pipe of the tee, and an oscillating flow source at the end of the latral pipe. It was revealed that the pumping effect in this type of system is such that pressure energy corresponding to the difference between the averages of kinetic energy in both sides of the main pipe and to the energy loss at the tee and at the end of the main pipe is stored in one of the tanks. The discussion in the previous paper was confined to the case when restoring force terms can be neglected, that is, resonance does not occur.

H.J.Bredow made experiments using flexible pipes and revealed that the subtraction of water levels in two tanks changes its sign periodically with an increase of the frequency of the oscillating flow source[(4)]. This phenomenon is considered to be related to the resonance of an infinite degree of freedom system. However, its details and mechanism have not been made clear yet.

In this paper, we modify a pump studied in the previous paper to such a form that resonance occurs in low frequency range, and discuss the effect of the resonance on pump characteristics theoretically and experimentally. The discussion is also confined to the case that the time average of flow in pipes is zero.

* Received 6th May, 1983.
** Associate Professor, Department of Energy Engineering, Toyohashi Univ. of Technology, Toyohashi 440, Japan.
*** Engineer, Nihon Denki Co., Ltd., Fuchu 183, Japan.

2. Mathematical model

2.1 Steady state flow characteristics at tee

Figure 1 shows the dimensions of a tee with a circular cross sectional area used in the experiment, which was made of transparent acrylic resin by machining. We represent the flow characteristics at the tee in the same form as in the

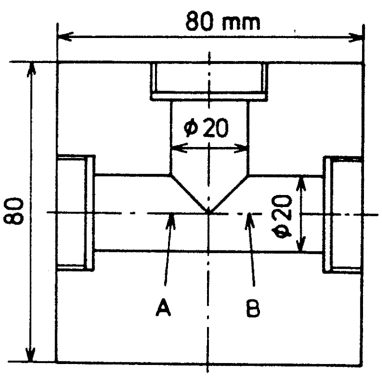

Fig. 1 Dimensions of the tee used

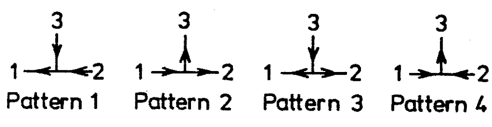

Fig. 2 Flow patterns at the tee

previous paper(6). For the four flow patterns shown in Fig.2, the pressure difference (P_1-P_2) is

$$P_1-P_2=(\rho/2A^2)(Q_2^2-Q_1^2\mp\zeta_{12}Q_m^2\,\mathrm{sgn}\,Q_3) \quad \cdots\cdots(1)$$

where $Q_i(i=1,2,3)$: the volume flow in the ith branch in Fig.2, whose positive direction is a direction denoted by the arrow in pattern 3 in Fig.2, $Q_m=\max\{|Q_1|,|Q_2|,|Q_3|\}$, ρ: density of fluid, A: cross sectional area of pipe, d: diameter of pipe, sgn:sign function, and the upper sign of the double sign corresponds to the case of $|Q_1|>|Q_2|$ and the lower one to $|Q_1|<|Q_2|$. The loss coefficient ζ_{12} is shown in Fig.3 against the flow ratio $|Q_j/Q_k|(|Q_k|>|Q_j|$, $j,k=1,2,j\neq k)$. The lines in Fig.3 were calculated from the experimental date for Reynolds number $R_e=(1\sim2)\times10^5$ by Ito and Imai(7).

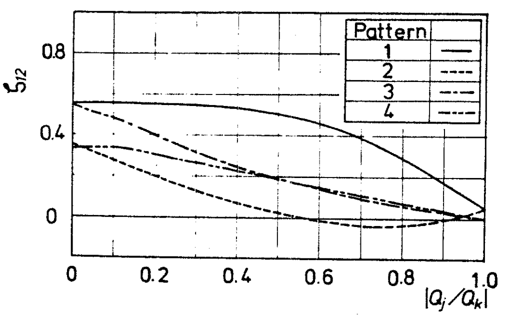

Fig. 3 Coefficients of head loss at tees

2.2 Fundamental equations

A schematic diagram of the system under study is shown in Fig.4. Two capacities are connected with both ends of the rigid main pipe of the tee and the oscillating flow is delivered to the lateral pipe by the piston. The capacities have closed air chambers. The restoring effect of the closed air contributes to the resonance phenomenon in the system. In Fig.4 S is the piston amplitude, ω the angular frequency, t the time, Q_i the volume flow in the ith branch where i=1,2, P_i, P_{ci} and P_{ti} the absolute pressures at the position indicated in Fig.4, P_{ai} the absolute pressure in the air chamber, V_i the volume of the air chamber, S_i the cross sectinal area of the capacity, Y_i the liquid level and l_i the pipe length where $l_1\geqq l_2$.

In this section we modify the mathematical madel proposed in the previous paper to such a form that the system has restoring terms and resonates under the following assumption:

(1) The liquid is incompressible.
(2) The law of pipe friction and flow characteristics at the tee for the steady state are applicable to the unsteady state.
(3) S_i is larger than A enough to be able to neglect the inertia of the liquid in the capacities.
(4) Adiabatic change occurs in the air chambers.
(5) The displacement of the piston is so small that the volume change of the air chamber is much less than the volume of the air chamber.

The continuity equation and the momentum equation are

$$Q_1+Q_2=SA_p\omega\cos\omega t \quad \cdots\cdots(2)$$

$$m_i\dot{Q}_i+4(l_i/d)\tau_i\mathrm{sgn}\,Q_i=P_i-P_{ci}(i=1,2) \quad \cdots\cdots(3)$$

where $m_i=\rho l_i/A$, A_p is the cross sectional area of the piston, τ_i the wall shearing stress, and a dot denotes differetiation with respect to t. The wall shearing stress is

$$\tau_i=(\rho/8A^2)\lambda_iQ_i^2 \quad \cdots\cdots(4)$$

where λ_i is the friction factor and is given as follow:

For laminar flow

$$\lambda_i=64/(|Q_i|d/A\nu) \quad \cdots\cdots(5)$$

For turbulent flow

$$\lambda_i=0.3164/(|Q|d/A\nu)^{0.25} \quad \cdots\cdots(6)$$

The relations at the capacities are

$$S_i\dot{Y}_i=Q_i \quad \cdots\cdots(7)$$

$$P_{ti}=P_{ai}+\rho gY_i \quad \cdots\cdots(8)$$

$$P_{ai}V_i^{\kappa}=P_{a0i}V_{0i}^{\kappa} \quad \cdots\cdots(9)$$

$$(Y_i-Y_{oi})S_i=V_{oi}-V_i \quad \cdots\cdots(10)$$

where g is the acceleration of gravity, κ the specific heat ratio of air, Y_{oi} P_{aoi} and V_{oi} are the liquid level, the absolute pressure and the air volume in the ith capacity for initial setting state, respectively. The initial setting state is the one in which the piston rests at the neutral position and the fluids are in equilibrium state.

At the tank ends of the main pipe the following equation holds.

$$P_{ci}=\begin{cases}P_{ti} & (Q_i\geqq0)\\ P_{ti}-(\rho/2A^2)(1+\zeta_t)Q_i^2 & (Q_i<0)\end{cases} \quad \cdots\cdots(11)$$

where ζ_t is the loss coefficient for the flow from the tanks to the pipes. An equation for the flow characteristics at the tee is Eq.(1).

Small deviations v_i and p_{ai} about the initial setting values V_{oi} and P_{aoi} are introduced, that is

$$v_i=V_i-V_{oi},\ p_{ai}=P_{ai}-P_{aoi} \quad \cdots\cdots(12)$$

From the assumption (5), we obtain $v_i\ll V_{oi}$ and $p_{ai}\ll P_{aoi}$.
Therefore Eq.(9) leads to

$$p_{ai}=-(\kappa P_{aoi}/V_{oi})v_i \quad \cdots\cdots(13)$$

Equations (1)∿(8),(10)∿(13) are the fundamental equations of the system.

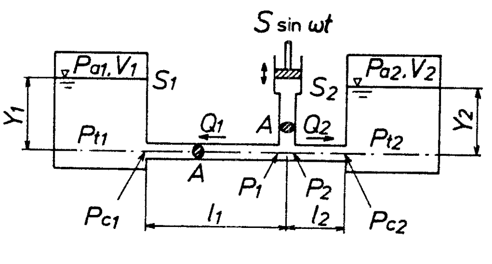

Fig. 4 Schematic diagram of the system under study

2.3 Zero discharge characteristics

The fundamental equations derived in the section 2.2 have complex nonlinear teams, and so it may be impossible to solve the fundamental equations in general. The flow pattern at the tee in operation can not be estimated either, because the phase of the fluid motion in the main pipe should depend on the frequency. Therefore in this section the zero discharge characteristics are discussed on the assumption that the energy loss at the tee can be neglected and the volume flows vary sinusoidally with the time. The volume flows Q_1 and Q_2 can be expressed as

$$Q_i = Q_{io}\sin(\omega t + \delta_i) \quad (i=1,2) \cdots\cdots\cdots\cdots(14)$$

where Q_{io} and δ_i are contants. Substituting Eq.(14) into Eqs.(1),(3),(11) and averraging both sides of these equations with respect to the time, we obtain

$$\Delta H = (\rho/8A^2)(1-\zeta_t)(Q_{2o}^2 - Q_{1o}^2) \cdots\cdots\cdots\cdots(15)$$

where $\Delta H(=\bar{P}_{t1}-\bar{P}_{t2})$ is the head for the zero discharge condition, $\bar{P}_{ti}$ is the time average value of P_{ti}. After examining Eq. (15), we reach the following conclusions:

(1) The time average of pressure in one of the capacities, which is connected with the pipe having a smaller flow amplitude, is larger than that in the other when $\zeta_t < 1$. However, the latter becomes larger when $\zeta_t > 1$.

(2) The absolute value of ΔH increases in proportion to the increase of the difference between the flow amplitude in the 1st pipe and the one in the 2nd pipe.

3. Experiment and discussion

3.1 Experimental set-up and method

The arrangement of an experimental set-up is schematically shown in Fig.5. The water tanks with an air chamber are installed at both ends of the main pipe of the tee (see Fig.1). The lateral pipe is connected with a cylinder through the nozzle and a polyvinyl chloride resin pipe with inner diameter of 4 cm. The sinusoidal oscillating flow is delivered in the lateral pipe by use of the piston which is driven by a motor with a stepless speed change device through a scotch yoke device. The main and the lateral pipes were composed of brass pipes and installed on the same horizontal plane. Two water tanks with the same geometry and dimensions were used. The screens were placed in the water tanks to prevent the water from sloshing. The entrances from the tanks to the main pipe with a radius of curvature of 1.25 cm were used in order to make the entrance loss coefficient ζ_t small.

We obtained the initial setting state of the apparatus by the following procedure: First the piston was kept at the neutral position. Second, after filling the cylinder, the pipe and the tanks with water, we discharged $2V_o$ cm^3 of water to obtain air chambers of volume V_o in both the tanks. Finally the air in the air chambers was compressed to a certain absolute pressure P_o and the valves B in Fig.5 were closed.

Pressures P_{t1} and P_{t2} in the tanks were measured by the pressure transducer P.T. in Fig.5. Water temherature was measured by a thermometer set in the 2nd tank. The dimensions of the apparatus and the condition of experiment are summarized in Table 1.

3.2 Experimental results and consideration

In this section we compare analytical results obtained from the mathematical model with those from experiment, discuss the validity of the model, and clarify the effect of resonance on pump characteristics.

3.2.1 Natural frequency of the system

Setting the displacement of the piston and all of the damping terms in the fundamental equation at zero, we obtain

$$(m_1+m_2)\ddot{Q}_1 + (K_1+K_2)Q_1 = 0 \cdots\cdots\cdots\cdots(16)$$

where $K_i = \kappa P_{oi}/V_{oi} + \rho g S_i$ (i=1.2). From Eq. (16) the natural frequency of the system is derived as

$$f_n = (1/2\pi)\sqrt{(K_1+K_2)/(m_1+m_2)} \cdots\cdots\cdots(17)$$

For the apparatus used, $P_{o1}=P_{o2}=P_o$, $V_{o1}=V_{o2}=V_o$ and $S_1=S_2=At$ hold, and so Eq. (17) reduces to

$$f_n = (1/2\pi)\sqrt{2K/(m_1+m_2)} \cdots\cdots\cdots\cdots(18)$$

where

$$K = \pi P_o/V_o + \rho g/A_t \cdots\cdots\cdots\cdots(19)$$

3.2.2 Pumping effect and resonance

In this sub-section we describe phenomena occurring in the system when the piston is driven with frequency in the neighborhood of f_n. An example of measured wavefoms with frequency adjacent to the resonance point of the system is given in Fig.6, where x is the displacement of the piston, p_{t1} and p_{t2} are the deviations of the pressure P_{t1} and P_{t2} about the initial setting state. As seen from the figure, the fundamental component of the waveforms is predominant. This proves validity of

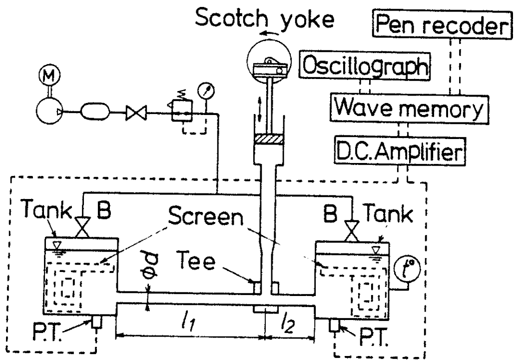

Fig. 5 Schematic diagram of the experimental set-up

Table 1 Dimensions of the apparatus and condition of experiment

Conduit	Diameter		d	2	cm
	Length		l_1	55∿70	cm
			l_2	10∿25	cm
Tank	Cross sectional area		A_t	402	cm^2
	Capacity			7799	cm^3
	Initial setting of air	Volume	V_o	1330∿2613	cm^3
		Pressure	P_o	121	kPa
Piston	Cross sectional area		A_p	28.27	cm^2
	Amplitude		S	1.15∿1.75	cm
	Frequency		f	0.455∿2.87	Hz

the prerequisite for the analysis in section 2.3 when the system operates in the neighborhood of the resonance point.

Figure 7 shows comparison of the experimental results with the computed ones using the fundamental equations. Pipe friction factors for laminar flow and for turbulent flow were used to obtain the computed results. Figure 7(a) shows the computed dimensionless amplitudes of flow in the main pipe R_{e1} and R_{e2} against the dimensionless frequency Ω' ($=f/f_n$), where

$$R_{ei}=U_i d/\nu \quad (i=1,2) \qquad \cdots\cdots(20)$$

and U_i is the amplitude of mean velocity averaged over the main pipe cross section. The solid line C.L. in Fig.7(a) represents

$$R_{ec}=441\sqrt{2\pi f d^2/\nu} \qquad \cdots\cdots(21)$$

Equation (21) gives the critical Reynolds number for oscillating flow; that is, when R_{ei} exceeds R_{ec} and $\sqrt{2\pi f d^2/\nu}>14$ holds, friction factors are given by Blasius's formula approximately(8). All measurements in this study were made under the condition that $\sqrt{2\pi f d^2/\nu}>14$ holds. In Fig.7(a) it is seen that the velocity amplitude R_{e1} in the longer pipe has a peak at the frequency a little lower than the natural frequency f_n and R_{e2} in the shorter pipe at the frequency a little higher than f_n. The amplitudes R_{ei} are larger than R_{ec} in the frequency range where a discrepancy between the two computed lines exists. Thus the computed line using the pipe friction factor for turbulent flow is reasonable in such an operational condition as shown in Fig.7. Figure 7(b) shows the computed lines and the measured value of the pressure amplitudes P_{ta1} and P_{ta2} of the pressures P_{t1} and P_{t2} in the two tanks. The peaks of P_{tai} corresponding to the peaks of R_{ei} come at the frequencies in the neighborhood of $\Omega'=1$.

Figure 8 shows the measured head ΔH with the computed lines for the same experimental condition as in Fig.7. In the frequency range $\Omega'<1$ the head ΔH is negative, that is, the time average pressure in the tank connected with the shorter pipe is higher than the one connected with the other side. However, the pressure in the tank connected with the longer pipe is higher when $\Omega'>1$. Referring to Fig.7(a), it is clear that the time average of pressure in the tank connected to the pipe with the smaller velocity amplitude is higher than that in the other one. And the head becomes larger in proportion to the difference between the velocity amplitudes. These results are in good agreement with the analytical ones (1) and (2) in the section 2.3.

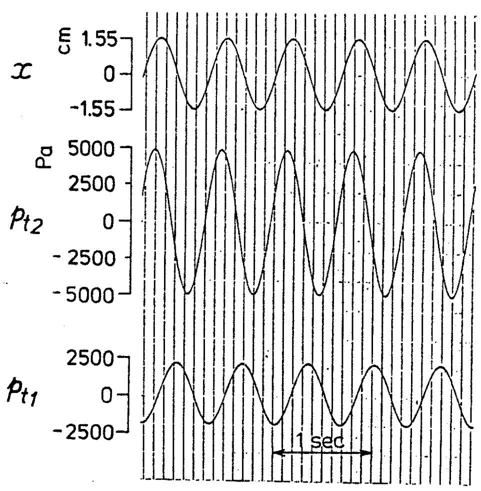

$S=1.55$ cm, $V_0=1\,809$ cm^3, $l_1=55$ cm, $l_2=25$ cm, $f_n=1.37$ Hz, $f=1.50$ Hz

Fig. 6 An example of measured waveforms

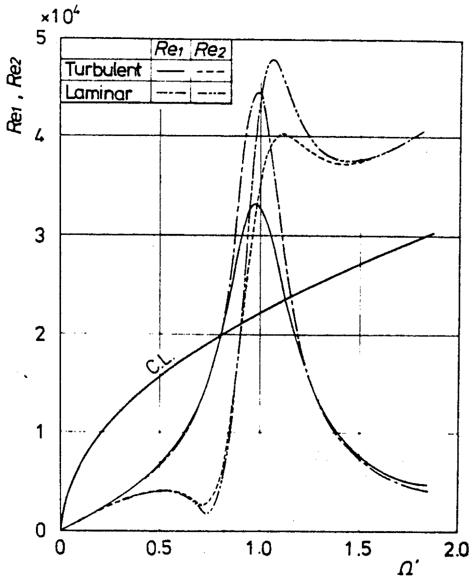

(a) Amplitudes of flow vs. frequency curves

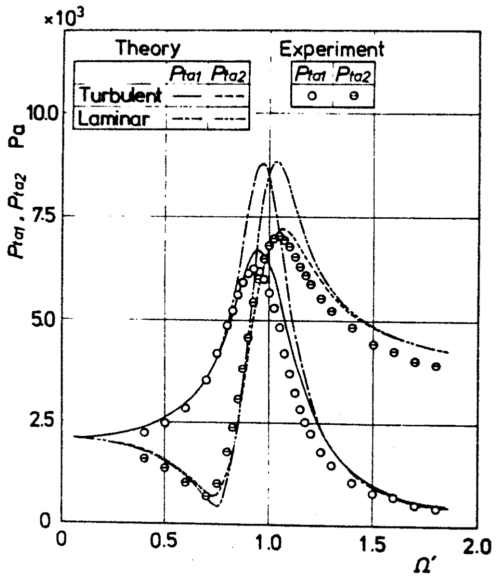

(b) Amplitudes of pressure in the tanks vs. frequency curves

$S=1.55$ cm, $V_0=1\,809$ cm^3, $l_1=70$ cm, $l_2=10$ cm, $f_n=1.37$ Hz

Fig. 7 Resonance curves

It is seen from Fig.7 and Fig.8 that the computed lines using the turbulent pipe friction agree with the measured values.

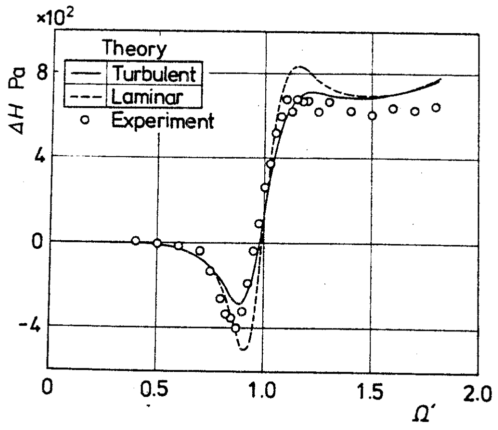

$S=1.55$ cm, $V_0=1\,809$ cm³, $l_1=70$ cm, $l_2=10$ cm, $f_n=1.37$ Hz

Fig. 8 Head versus frequency curves

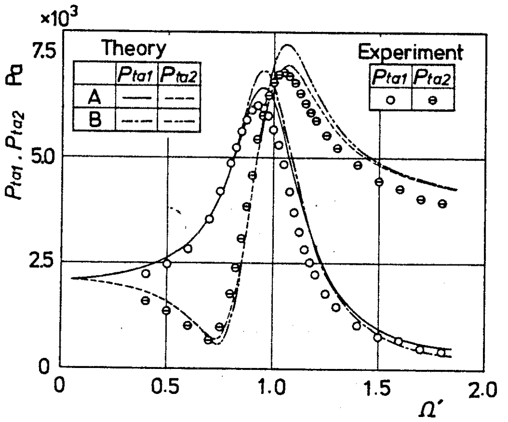

(a) Amplitudes of pressure in the tanks vs. frequency curves

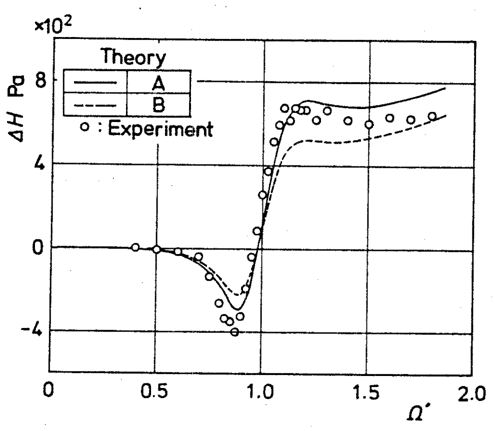

(b) Head versus frequency curves

$S=1.55$ cm, $V_0=1\,809$ cm³, $l_1=70$ cm, $l_2=10$ cm, $f_n=1.37$ Hz

Fig. 9 Effect of the loss at tees

Hereinafter only the computed lines using the turbulent pipe friction are shown.

Figure 9 shows an example of the effect of the loss of head at the tee on the P_{tai} versus Ω' curves and the ΔH versus Ω' curves. In the figure A denotes the computed curves which were derived from the curves of ζ_{12} in Fig.3, and B the ones when $\zeta_{12}=0$. The loss at the tee little affects P_{tai} but it does ΔH considerably.

The P_{tai} versus Ω' curves and the ΔH versus Ω' curves computed from the mathematical model are shown for three values of the water temperature (i.e. the values of kinematic viscosity) in Fig.10. The curves were computed under the assumption that the change of the viscosity causes only the change of the pipe friction. It is seen that the amplitudes of pressure in the tanks and the head depend a little on the change of the kinematic viscosity only in the neighborhood of the resonance point. The results obtained from Fig.10 (a) and Fig.9 (a) lead to the conclusion that one of all damping teams which affects the resonance phenomenon dominantly is the energy loss for the flow from the pipe to the tank when the pipe is short and the pipe friction is small.

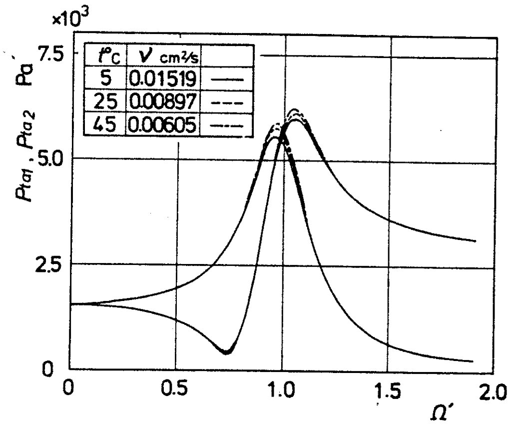

(a) Amplitudes of pressure in the tanks vs. frequency curves

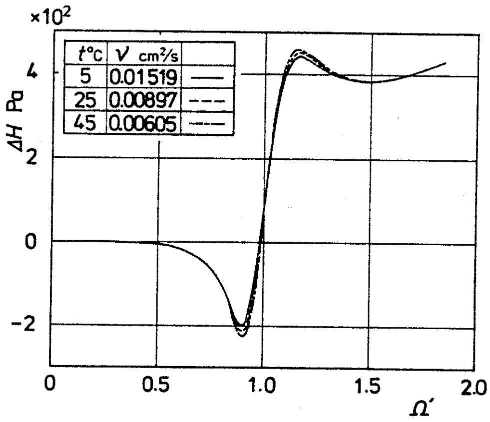

(b) Head versus frequency curves

$S=1.15$ cm, $V_0=1\,809$ cm³, $l_1=70$ cm, $l_2=10$ cm, $f_n=1.37$ Hz

Fig. 10 Effect of kinematic viscosity

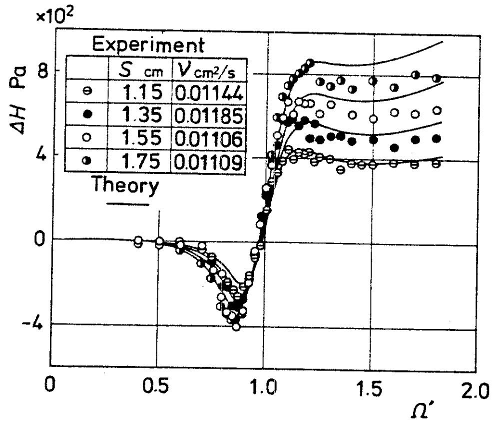

$V_0 = 1\,809\ cm^3$, $l_1 = 70\ cm$, $l_2 = 10\ cm$, $f_n = 1.37\ Hz$

Fig. 11 ΔH versus Ω' curves for the amplitude of piston

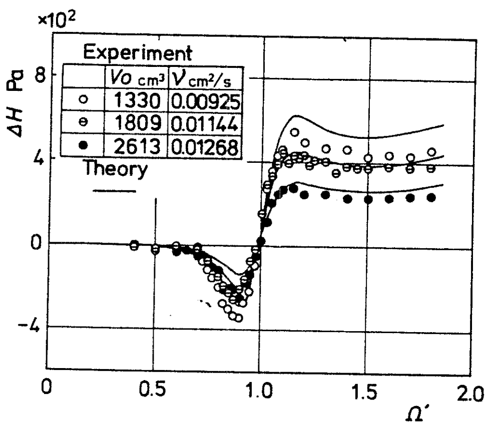

$S = 1.15\ cm$, $l_1 = 70\ cm$, $l_2 = 10\ cm$

Fig. 12 ΔH versus Ω' curves for the volume of air chambers

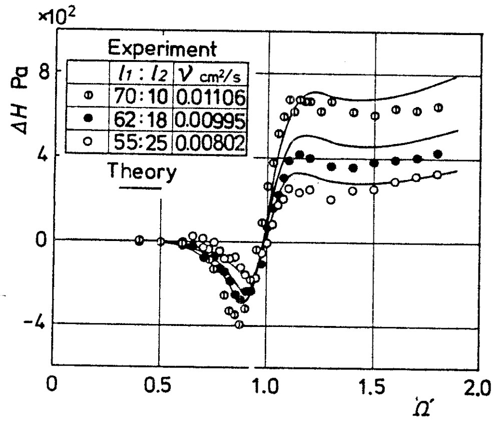

$S = 1.55\ cm$, $V_0 = 1\,809\ cm^3$, $f_n = 1.37\ Hz$

Fig. 13 ΔH versus Ω' curves for the ratio of pipe

In Fig.11 the measured ΔH versus Ω' curves and the computed ones are shown for four values of the piston amplitude S. The absolute value of ΔH increases with an increase of S, because the amlitude of flow in the lateral pipe is in proportion to S.

The ΔH versus Ω' curves are shown for the air chamber volume V_0 in Fig.12, and for the pipe length ratio l_1/l_2 in Fig.13 where the total length of the main pipe $l(= l_1 + l_2)$ is kept at 80 cm.

The analytical results using the mathematical model described hereinbefore are in good agreement with the measured ones. Therefore we conclude that the mathematical model applied in this paper represents well the pumping effect and the resonance occurring in the system.

4. Conclusions

The pumping effect and the resonance phenomenon occurring in a piston pump without valves, which consists of a rigid pipe system with a T-junction, two capacities connected with both ends of the main pipe and a piston installed in the lateral pipe, are studied theoretically and experimentally. The results are summarized as follow:

(1) The mean pressure in one of the capacities is higher than that in the other for the low frequency range, and becomes smaller for higher frequencies than a certain value close to the resonance frequency.

(2) The pumping effect increases with an increase of the difference between the amplitudes of velocity in the main pipe connected with both sides of the tee.

(3) The effect of the loss of head at the tee and the pipe friction as the damping terms on the amplitude of velocity in the pipes is smaller for the experimental condition in this paper. The pipe friction hardly contributes to the pump characteristics but the loss of head at the tee considerably does.

(4) The mathematical model used in this paper predicts well the pumping effect and the resonance phenomena.

References

(1) Liebau, G., Z. ges. exp. Medizin, 123-1(1954), 71.
(2) Liebau, G., Naturwiss., 41-14(1954), 327.
(3) Liebau, G., Z. ges. exp. Medizin, 125-5(1955), 482.
(4) Bredow, H., J., Fortschr.-Ber., VDI-Z, 7-9(1968).
(5) Mahrenholtz, O., Forsch. Ing.-wess., 29-2(1963), 47.
(6) Takagi, S. and Saijo, T., Bull. of the JSME, 26-218(1983-8), 1366.
(7) Ito, H. and Imai. K., Proc. Amer. Soc. Civ. Engrs., 99-HY9, (1973-9), 1353.
(8) Ohmi, M. and Iguchi, M., Trans. JSME (in Japanese), 47-418, B(1981-6),993.